ELSEVIER

Journal of Molecular Catalysis A: Chemical 112 (1996) 269–276

JOURNAL OF MOLECULAR CATALYSIS A: CHEMICAL

Oxidation of S(IV) to S(VI) under Fenton, photo-Fenton and γ-FeOOH photocatalized conditions

Anas Ansari [a], José Peral [a], Xavier Domènech [a,*], Rafael Rodríguez-Clemente [b], Juan Casado [c]

[a] *Departament de Química, Universitat Autònoma de Barcelona, 08193 Bellaterra, Spain*
[b] *Institut de Ciències dels Materials de Barcelona, CSIC, 08193 Bellaterra, Spain*
[c] *Carburos Metálicos, S.A., Pº Zona Franca, 14–20, 08038 Barcelona, Spain*

Received 15 August 1995; accepted 19 January 1996

Abstract

Hydrogen sulphite oxidation to sulphate through three different routes was investigated. Fenton and photo-Fenton reactions were used to carry out the oxidation process. γ-FeOOH was also used in order to promote the photocatalytic oxidation of S(IV) species. In all three cases a kinetic model based on an autocatalytic reaction is suggested to account for the experimental results obtained. According to this model the intermediate species HSO_5^- and/or $SO_5^{\cdot-}$, generated during S(IV) oxidation, should be involved in the autocatalytic mechanism.

Keywords: Oxidation; Sulphur; Fenton reactions; Photocatalysis; Iron; Peroxide

1. Introduction

The chemistry involved in the gas-phase oxidation of S(IV) to S(VI) species is a subject of interest because it gives insight into the processes that generate the acid rain in the atmosphere [1]. It is accepted that SO_2 is mainly oxidized in the aqueous phase [2]. In this way the anions HSO_3^- and SO_3^{2-}, formed by the dissolution of SO_2 in the atmospheric water droplets, are oxidized to H_2SO_4 [2]. Different mechanisms have been proposed to account for the oxidation of S(IV) species, those most accepted are those taking place homogenously and involving the participation of radical species like $HO_2^{\cdot}$, $O_2^{\cdot-}$ or $HO^{\cdot}$, or those which involve catalysis by trace metal impurities present in water [3]. Other authors have indicated the occurrence of heterogeneous processes where the surface of atmospheric particulate matter acts as catalyst for the S(IV) species oxidation [4–7]. Although it is accepted that the $HO^{\cdot}$ radicals are mainly formed by ozone initiated reactions, other species present in atmospheric water like H_2O_2, Fe(II), Fe(III) and semiconductor particles as iron oxides, can be also responsible for the oxidation of S(IV) to S(VI) through chemical and photochemical reactions. However, the role that these species play in such processes is still not clear. In this paper are presented the results of a laboratory study of the aqueous oxidation of HSO_3^- at pH = 3. We have used Fenton

* Corresponding author.

PII S1381-1169(96)00043-X

(Fe(II) + H_2O_2) and photo-Fenton (Fe(III) + $h\nu$) reagents, and a heterogeneous photocatalyst γ-FeOOH (which is present in natural environments [8]). These oxide species are semiconductors capable of photo-excitation after absorption of sunlight. The electrons and holes generated in this way, after migrating to the particle surface, can react with species in solution of suitable redox potential. The reaction of holes and/or electrons with water and HO^- ions is a generally accepted way of generating $HO^{\cdot}$ radicals, which remain adsorbed onto the semiconductor surface [9]. The aim is to create conditions suitable for radical chain reactions through homogeneous catalysis initiated by metal traces, or through heterogeneous catalysis onto a solid particle surface. The concentrations of H_2O_2 chosen in the experiment were below 10^{-4} M in order to mimic natural processes. From the results obtained a kinetic model for S(IV) oxidation to S(VI) is discussed and the three routes of oxidation are compared.

2. Experimental section

All chemicals used were of reagent grade. Na_2SO_3, $FeCl_2$ and $FeCl_3$ were used as the sulphite, Fe(II) and Fe(III) sources, respectively. The γ-FeOOH was synthesized from a $FeCl_2$ solution following the procedure described by Domingo [10]. X-ray diffraction analysis of the solid using a Siemens D500 diffractometer gave well defined crystalline parameters, which were confirmed by Mössbauer spectroscopy. The mean particle size and the specific surface area of the iron oxo-hydroxide sample were 171 nm and 127.5 $m^2\ g^{-1}$ respectively. The mean particle size was determined visually by scanning electron microscopy (Hitachi S-570 microscope) and the specific surface area was measured by BET analysis with a Micromeritics ASAP-2000 apparatus. The ^{57}Fe transmission Mössbauer spectra were recorded with a 512 multichannel analyzer coupled to a constant acceleration drive. A proportional Xe gas mixture counter was used to detect the radiation. The γ-ray source was ^{57}Co doped in a Rh matrix. The spectrometer was calibrated with an α-Fe foil of 25 μm thickness. The obtained data were folded and then fitted using a least-squares program. The point of zero charge of γ-FeOOH was 3.9.

The photocatalytic experiments were performed in an open (aerated) thermostated cylindrical Pyrex cell of 100 ml volume. The suspension was stirred magnetically. A 250 xenon lamp (Applied Photophysics) was used as light source. The IR fraction of the light beam was removed by the water in the double jacket of the photoreactor. The intensity of the incident light inside the cell, measured employing a uranyl oxalate actinometer, was 6×10^{-6} Einstein min^{-1}. All experiments were carried out at 25 ± 0.1°C. The analyses of iron species and H_2O_2 in solution were performed using polarography (Metrohm 626) with background solutions of 0.1 mol l^{-1} NaCl and 0.1 mol l^{-1} NH_3/NH_4^+ buffer, respectively. The concentration of sulphite was determined by means of the reaction between sulphite and a disulphide (5,5′-dithiobis-2-nitrobenzoic acid) which generate a thiol that can be analysed using visible spectroscopy [11].

3. Results and discussion

3.1. Oxidation by the Fenton reagent

The oxidation of bisulphite (HSO_3^-) to sulphate at pH ≈ 3 was first carried out by means of the traditional Fenton reagent. It is well known that a Fe(II) salt mixed with H_2O_2 in aqueous solutions generates hydroxyl radicals ($OH^{\cdot}$) [12], an extremely strong and non-selective oxidant ($E^0_{HO^{\cdot}} = 2.86$ V vs. SHE), which readily reacts with HSO_3^-, producing the SO_3^{-} radical, which eventually evolves to SO_4^{2-}, as will be seen later.

$$Fe(II) + H_2O_2 \rightarrow Fe(III) + HO^{\cdot} + HO^- \quad (1)$$

$$HO^{\cdot} + HSO_3^- \rightarrow H_2O + SO_3^{-} \quad (2)$$

The change of HSO_3^- concentration with reaction time for an initial aqueous solution of 0.005 mol l^{-1} HSO_3^- at pH ≈ 3 is shown in Fig. 1, both in absence and presence of Xe light. The initial concentration of Fe(II) and H_2O_2 used in these experiments were 2×10^{-4} mol l^{-1} and 2.5×10^{-5} mol l^{-1}, respectively. As can be seen, an initial activation time (20 min in the most favourable case) is needed for the detection of a noticeable change in HSO_3^- concentration. For the rest of the text, and due to the error associated to the measurements of activation time from $[HSO_3^-]$ vs. time data, it will be quantified by means of the half-life ($t_{1/2}$). After the activation period the reaction rate rapidly increases arriving at a maximum value, which seems to be independent of the initial experimental conditions. For longer times the reaction rate decreases, going back to zero. The amounts of Fe(II) and H_2O_2 used are not sufficient to allow complete stoichiometric destruction of all HSO_3^- ions initially present, if the Fenton reaction with the HO· radicals is to be the only acting mechanism. This indicates that the reaction takes place through a catalytic mechanism involving consumption of O_2. On the other hand, the use of Xe light for the excitation of the H_2O_2 molecules only slightly improves the reaction rate, as compared with the use of H_2O_2 alone, leading to a decrease of $t_{1/2}$. Indeed, the absorption spectra of the different reactants (HSO_3^-, H_2O_2 and Fe(II)) at the concentrations used through the study showed no noticeable photoactivity. Only when the three of them are mixed, does the solution develop a light yellow color, whose UV–Vis spectrum matches the absorption of Fe(III) in solution. Fig. 1 also shows the reactivity of HSO_3^- in presence of H_2O_2 and absence of Fe(II). For those experimental conditions the system obeys a similar kinetic pattern, the most remarkable difference being the large increase of $t_{1/2}$ relative to those in the presence of Fe(II), and the beneficial effect of Xe light radiation. Due to the absence of Fe(II), the data are consistent with the hypothesis that the Fenton reaction is not the only possible reaction pathway for HSO_3^- oxidation. As will be discussed later, the profiles of the kinetic curves in Fig. 1 resemble those of an autocatalytic system. The solid lines show the curve fitting of the experimental data to the kinetic equation.

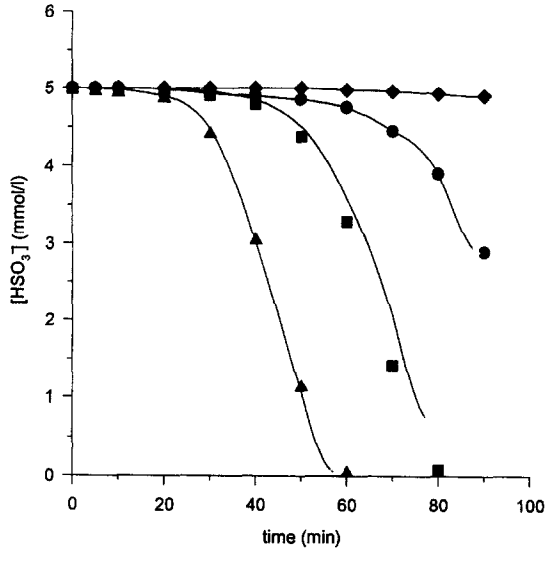

Fig. 1. Time course of HSO_3^- concentration for different experimental conditions: (a) in presence of Xe light and Fe(II) (▲), (b) in presence of Fe(II) and absence of Xe light (■), (c) in presence of Xe light and absence of Fe(II) (●), and (d) in absence of both Xe light and Fe(II) (◆). $[HSO_3^-]_0 = 5 \times 10^{-3}$ mol l^{-1}, $[Fe(II)]_0 = 2 \times 10^{-4}$ mol l^{-1}, $[H_2O_2]_0 = 2.5 \times 10^{-5}$ mol l^{-1} and $pH_0 \approx 3$.

3.2. Oxidation by the photo-Fenton reagent

Another possible mechanism of reaction for HSO_3^- oxidation that involves an iron aqueous salt is the photo-Fenton reaction [13]. Fe(III) ions in aqueous solution, after hydrolysis (Eq. 3), absorb a photon, giving a HO· radical (Eq. 4) which in turn oxidizes HSO_3^- (Eq. 2):

$$Fe^{3+} + H_2O \rightarrow FeOH^{2+} + H^+ \quad (3)$$

$$FeOH^{2+} + h\nu \rightarrow Fe^{2+} + HO^{\cdot} \quad (4)$$

The time course of the HSO_3^- concentrations for different experimental conditions is depicted in Fig. 2. The same sigmoidal profile of the Fenton systems, reported in Fig. 1, is observed

for this new experimental situation. The value of $t_{1/2}$ for the most favourable case (Fe(III) + H_2O_2 + Xe light) is 40 min (see Table 1). For all other cases $t_{1/2}$ has values between 62–67 min, which means longer activation times before detecting the reaction. For the whole set of curves the maximum slope, which corresponds to the largest reaction rate, is within a narrow range (see apparent reaction rate constants in Table 1). Thus, as in the Fenton systems, once the activation period is over and the reaction has initiated, the evolution of HSO_3^- is independent of the initial conditions, and proceeds even in the absence of H_2O_2.

3.3. Oxidation by a photocatalytic system

Another possible reaction pathway for HSO_3^- oxidation involves the use of an iron oxide slurry. The main role that different crystalline forms of Fe_2O_3 and FeOOH play in the oxidation of SO_2 in natural environments has been reported by other authors [7,14]. We have chosen γ-FeOOH as a model catalyst for the study of the HSO_3^- reaction. Eqs. 5–8 describe the fundamental steps involved in such a direct photocatalytic process. The $HO^{\cdot}$ radicals formed in reaction 8 may react in solution with $HSO_3^{\cdot -}$ as described in Eq. 2.

$$\gamma\text{-FeOOH} + h\nu \rightarrow \gamma\text{-FeOOH}(h^+ - e^-) \quad (5)$$

$$h^+ \xrightarrow[\text{migration}]{\text{surface}} (Fe^{3+}\text{–}O^{\cdot -}\text{–}Fe^{3+}) \quad (6)$$

$$(Fe^{3+}\text{–}O^{\cdot -} - Fe^{3+}) \quad O_{3_{ads}}^{-}S \rightarrow (Fe^{3+} - O^{2-} - Fe^{3+}) + HSO_{3_{ads}}^{\cdot} \quad (7)$$

$$(Fe^{3+}\text{–}O^{\cdot -}\text{–}Fe^{3+}) + OH_{ads}^{-} \rightarrow (Fe^{3+}\text{–}O^{2-}\text{–}Fe^{3+}) + OH_{ads}^{\cdot} \quad (8)$$

Iron oxo-hydroxides have been shown to interchange Fe species with the solution [15] due to

Table 1
Reaction rate constants and $t_{1/2}$ of HSO_3^- oxidation under different experimental conditions. The constants have been calculated by curve fitting to Eq. 9

Initial conditions	k_{cal} (l mol^{-1} min^{-1}) × 10^5	$t_{1/2}$ (min)
H_2O_2 (25 mM)/HSO_3^- (5 mM)/Xe light	1.6	90
Fe(III) (0.2 mM)/HSO_3^- (5 mM)	2.9	67
Fe(III) (0.2 mM)/HSO_3^- (5 mM)/Xe light	3.4	62
Fe(III) (0.1 mM)/H_2O_2 (0.25 mM)/HSO_3^- (5 mM)/Xe light	3.0	40
Fe(III) (0.2 mM)/H_2O_2 (0.25 mM)/HSO_3^- (5 mM)/Xe light	2.8	48
Fe(III) (0.1 mM)/H_2O_2 (0.25 mM)/HSO_3^- (5 mM)	3.2	64
Fe(III) (0.2 mM)/H_2O_2 (0.25 mM)/HSO_3^- (5 mM)	2.9	42
Fe(II) (0.2 mM)/H_2O_2 (0.25 mM)/HSO_3^- (5 mM)/Xe light	2.3	42
Fe(II) (0.2 mM)/H_2O_2 (0.25 mM)/HSO_3^- (5 mM)	2.3	65
γ-FeOOH/HSO_3^- (5 mM)	2.2	51
γ-FeOOH/HSO_3^- (5 mM)/Xe light	3.8	45
γ-FeOOH/H_2O_2 (0.25 mM)/HSO_3^- (5 mM)/Xe light	3.4	38
γ-FeOOH/H_2O_2 (0.1 mM)/HSO_3^- (5 mM)/Xe light	4.0	43
γ-FeOOH/H_2O_2 (0.01 mM)/HSO_3^- (5 mM)/Xe light	2.8	44
γ-FeOOH/H_2O_2 (0.25 mM)/HSO_3^- (5 mM)	2.6	52
γ-FeOOH/H_2O_2 (0.1 mM)/HSO_3^- (5 mM)	1.9	61
γ-FeOOH/H_2O_2 (0.01 mM)/HSO_3^- (5 mM)	2.3	66
γ-FeOOH/H_2O_2 (0.1 mM)/HSO_3^- (5 mM)/N_2	2.7	51
γ-FeOOH/Fe(II) (0.2 mM)/HSO_3^- (5 mM)	2.1	64
γ-FeOOH/Fe(II) (0.8 mM)/HSO_3^- (5 mM)	2.9	57
γ-FeOOH/Fe(II) (2 mM)/HSO_3^- (5 mM)	1.6	54
γ-FeOOH/Fe(II) (0.2 mM)/HSO_3^- (5 mM)/Xe light		44
γ-FeOOH/Fe(II) (0.8 mM)/HSO_3^- (5 mM)/Xe light	4.0	39
γ-FeOOH/Fe(II) (2 mM)/HSO_3^- (5 mM)/Xe light	3.7	40
γ-FeOOH/Fe(II) (0.2 mM)/H_2O_2 (0.25 mM)/HSO_3^- (5 mM)	2.3	52
γ-FeOOH/Fe(II) (0.2 mM)/H_2O_2 (0.25 mM)/HSO_3^- (5 mM)/Xe light	3.8	42

corrosion and photo-corrosion reactions, therefore providing the parallel occurrence of photocatalytic, Fenton and photo-Fenton mechanisms. Data corresponding to the time course of HSO_3^- solutions at different initial experimental conditions and in the general frame of a photocatalytic system is plotted in Fig. 3. Again, the profiles of the curves are similar to each other and resemble those in Fig. 1 and Fig. 2, and, as will be seen shortly, they seem to be due to the occurrence of an autocatalytic process. The only difference among each set of data is the time needed for the system to build up the suitable concentration of some key intermediate that triggers the autocatalytic mechanism. In Fig. 3 the shortest $t_{1/2}$ is 36 min, which corresponds to the γ-FeOOH/H_2O_2 (0.25 mM)/HSO_3^- (5 mM)/Xe light system. As can be seen in Fig. 4 the longest induction times in each figure are those required for the systems either containing no iron species in solution or without irradiation. In general, comparing two systems with the same set of initial conditions and which

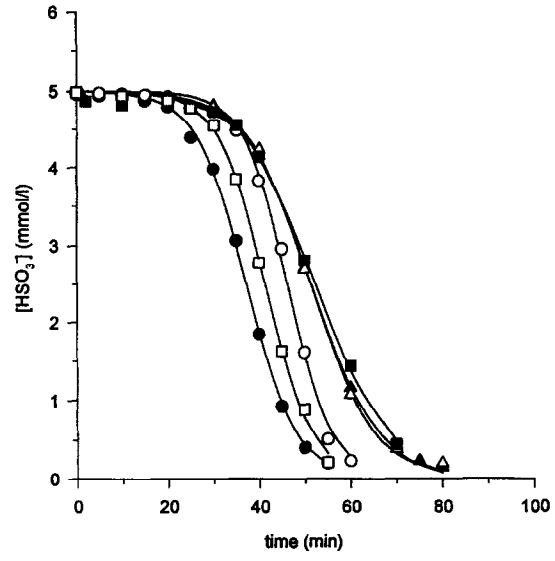

Fig. 3. Time course of HSO_3^- concentration for different experimental conditions in presence of γ-FeOOH: (a) in presence of Xe light and H_2O_2 (●), (b) in presence of Xe light, H_2O_2 and Fe(II) (□), (c) in presence of Xe light (○), (d) in presence of H_2O_2 and absence of Xe light (△), (e) in absence of Xe light (▲), and (f) in presence of H_2O_2 and Fe(II), but absence of Xe light (■). $[\gamma\text{-FeOOH}]_0 = 1.7$ g l^{-1}, $[HSO_3^-]_0 = 5\times10^{-3}$ mol l^{-1}, $[Fe(II)]_0 = 2\times10^{-4}$ mol l^{-1}, $[H_2O_2]_0 = 2.5\times10^{-5}$ mol l^{-1} and $pH_0 \simeq 3$.

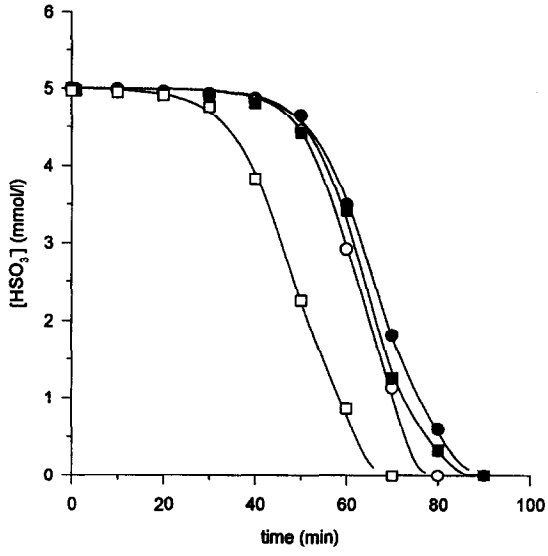

Fig. 2. Time course of HSO_3^- concentration for different experimental conditions in presence of Fe(III): (a) in presence of Xe light and H_2O_2 (□), (b) in presence of Xe light and absence of H_2O_2 (○), (c) in presence of H_2O_2 and absence of Xe light (■), and (d) in absence of both Xe light and H_2O_2 (●). $[HSO_3^-]_0 = 5\times10^{-3}$ mol l^{-1}, $[Fe(III)]_0 = 2\times10^{-4}$ mol l^{-1}, $[H_2O_2]_0 = 2.5\times10^{-5}$ mol l^{-1} and $pH_0 \simeq 3$.

differ only in the presence of irradiation, we found that the participation of Xe light produces shorter activation times (Fig. 4). The best results for each set of experiments are obtained when H_2O_2, light and an Fe species (we include here the γ-FeOOH) form part of the same system. A numerical treatment consisting of the curve fitting of the experimental data to the kinetic equation derived from an autocatalytic system has been carried out in order to ascertain the suitability of such a model [16]. Assuming that the oxidation of HSO_3^- produces an intermediate species I responsible for the autocatalysis:

$$HSO_3^- \xrightarrow{\text{oxidation}} I \qquad (9)$$

then, the equation that describes the solid lines of Figs. 1–3 would be [16]:

$$\frac{dx}{dt} = k([HSO_3^-]_0 - x)([I]_0 + x) \qquad (10)$$

x is the amount of HSO_3^- reacted at a time t

and I_0 is the concentration of I at time 0. Integration of Eq. 9 gives:

$$\frac{[HSO_3^-]_0 - [HSO_3^-]}{[I]_0} = \frac{\exp(k([HSO_3^-]_0 + [I]_0)t) - 1}{1 + \frac{[I]_0}{[HSO_3^-]}\exp(k([HSO_3^-]_0 + [I]_0)t)} \quad (11)$$

The curve fitting treatment also allows the calculation of the apparent reaction rate constants for the whole set of experimental situations studied in this paper, which are shown in Table 1. Eq. 10 does not strictly describe the data reported here, since at time 0 the concentration of I is zero. But considering that the initial delay times allow the build up of an appreciable amount of I, at some point in time the equation fully describes the kinetics of our different systems. In this way, each particular set of initial experimental conditions leads to different calculated values of $[I]_0$, those reactions with larger $[I]_0$ being faster.

The iron-catalyzed oxidation of HSO_3^- in aqueous solution has been studied by Warneck and coworkers [17–19]. They provide evidence for a free radical chain mechanism which is initiated with the formation of an HO· radical in a photo-Fenton reaction (Eqs. 3 and 4). The HO· radical reacts with HSO_3^- by the mechanism:

$$HO\cdot + HSO_3^- \rightarrow H_2O + SO_3^{-\cdot} \quad \text{(Eq.2)}$$

$$SO_3^{-\cdot} + O_2 \rightarrow SO_5^{-\cdot} \quad (12)$$

$$SO_5^{-\cdot} + HSO_3^- \rightarrow HSO_5^- + SO_3^{-\cdot} \quad (13)$$

$$HSO_5^- + HSO_3^- \rightarrow 2SO_4^{2-} + 2H^+ \quad (14)$$

eventually giving the SO_4^{2-} ion. Although several more steps are considered in the Warneck's mechanism, we report here only those needed to explain the autocatalytic kinetics. The intermediate species HSO_5^- or $SO_5^{-\cdot}$ from reactions 13

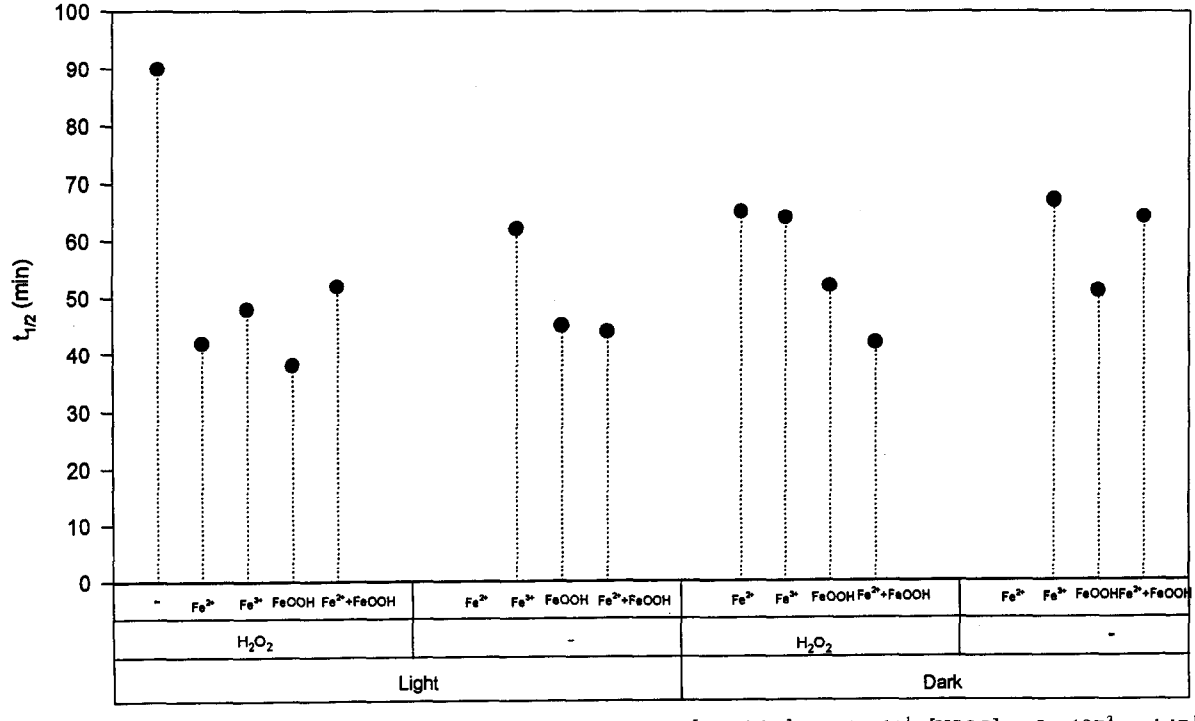

Fig. 4. Half-life of HSO_3^- oxidation in selected experiments from Table 1. $[\gamma\text{-FeOOH}]_0 = 1.7$ g l^{-1}, $[HSO_3^-]_0 = 5 \times 10^{-3}$ mol l^{-1}, $[Fe(II)]_0 = [Fe(II)]_0 = 2 \times 10^{-4}$ mol l^{-1}, $[H_2O_2]_0 = 2.5 \times 10^{-5}$ mol l^{-1} and $pH_0 \simeq 3$.

and 14, seem to be responsible for the autocatalytic mechanism, thus playing the role of I in Eqs. 9–11. One important consequence that can be derived from this mechanism is the fact that once the $HO^{\cdot}$ radical has been formed, the evolution of the system will be independent of the initial conditions, which is what we have found for three completely different experimental situations: Fenton, photo-Fenton and photocatalytic conditions. Each of these mechanisms produce $HO^{\cdot}$ radicals, which after reacting with HSO_3^- trigger the autocatalysis. The only difference between each set of experimental conditions listed in Table 1 appears during the first minutes of the reaction, and would again be explained by the ability to generate an appreciable amount of the HSO_5^- or $SO_5^{\cdot-}$ intermediate.

Another remarkable fact is the need for dissolved O_2 if the reaction is to be sustained, especially in the case of Fenton and photo-Fenton conditions, although in theory (see Eqs. 1–4) the presence of this oxidant is not required during the initial steps of either reaction pathway. Indeed, the experimental results show that O_2 in solution is a requirement except in the case of some photocatalytic reactions (see the γ-FeOOH/H_2O_2 (0.1 mM)/HSO_3^- (5 mM)/N_2 system in Table 1). The photocatalytic systems need the presence of species in solution with suitable redox potential and capable of accepting the electrons that accumulate in the conduction band upon irradiation [14]. O_2 normally plays this role for many semiconductors in aqueous environments. However, some iron oxides and oxo-hydroxides dispose of the excess of electrons by reducing the Fe(III) of their own crystalline structure and releasing Fe^{2+} ions in solution [15]. Warneck's mechanism can also be accepted as an explanation for the autocatalysis detected with the photocatalytic systems, except in the case mentioned above where the initiation of the reaction in absence of O_2 can be explained by the γ-FeOOH lattice iron reduction, but where other not identified reaction pathways have to apply for autocatalysis to be sustained in absence of O_2.

4. Conclusions

The oxidation of HSO_3^{2-} in Fenton, photo-Fenton and γ-FeOOH photocatalytic systems has shown to follow the same mechanism once activation time has passed. This activation time is necessary for the system to build up an appreciable amount of an intermediate, probably HSO_5^- or $SO_5^{\cdot-}$, which may be responsible for the occurrence of an autocatalytic process. The apparent kinetic constants calculated by the kinetic equation derived for an autocatalytic system are in a narrow range, even for a large set of different experimental conditions.

Acknowledgements

The authors thank the CICYT (Spanish Government) for funding the work done in this paper (Project MAT92-0263-C02-01).

References

[1] B.J. Pynlayson-Pitts and J.N. Pitts, Atmospheric Chemistry: Fundamentals and Experimental Techniques, Wiley, New York, 1986.
[2] P. Warneck, Chemistry of the Natural Atmosphere, Academic Press, San Diego, CA, 1988.
[3] D.A. Hegg and P.V. Hobbs, Atmos. Environ., 12 (1978) 241.
[4] J.G. Calvert, A. Larzus, G.L. Kok, B.G. Heikes, J.G. Walega, J. Lind and C.A. Cantrell, Nature, 317 (1985) 27.
[5] H. Hob, H. Elias and K. Wannowius, Atmos. Environ., 25A (1991) 1715.
[6] S.O. Pehkonen, R. Siefert, Y. Erel, S. Webb and M. Hoffmann, Environ. Sci. Technol., 27 (1993) 2056.
[7] B.C. Faust, M.R. Hoffmann and D. Bahnemann, J. Phys. Chem., 93 (1989) 6371.
[8] T. Fukasawa, M. Iwatsuki, S. Kawakubo and K. Miyazaki, Anal. Chem., 52 (1980) 1784.
[9] E. Pelizzetti and C. Minero, Electrochim. Acta, 38 (1993) 47.
[10] P. Domingo, Ph.D. Thesis, Universitat de Barcelona, Facultat de Química, January, 1992.
[11] R.E. Humphrey, M.H. Ward and W. Hinze, Anal. Chem., 42 (1970) 698.
[12] S.J. Masten and S.H.R. Davies, Environ. Sci. Technol., 28 (1994) 180.
[13] G. Ruppert, R. Bauer and G. Heisler, J. Photochem. Photobiol. A, 73 (1993) 75.
[14] A. Kotronarou and L. Sigg, Environ. Sci. Technol., 27 (1993) 2725.

[15] A. Ansari, J. Peral, X. Domenech, R. Rodriguez-Clemente, A. Roig and E. Molins, J. Photochem. Photobiol. A, 87 (1995) 121.
[16] P.W. Atkins, Physical Chemistry, 3rd Ed., Oxford University Press, 1986, p. 847.
[17] P. Warneck, Ber. Bunsenges. Phys. Chem., 96 (1993) 454.
[18] J. Ziajka, F. Beer and P. Warneck, Atmos. Environ., 28 (1994) 2549.
[19] P. Warneck, Fresenius J. Anal. Chem., 340 (1991) 585.